LA-UR-00-5848

Approved for public release; distribution is unlimited.

Title: **FISSION PRODUCT YIELDS IN HYBRID (ADS) TARGET MATERIALS INDUCED BY HIGH-ENERGY PROTONS**

Author(s): Yury E. Titarenko, Oleg V. Shvedov, Vyacheslav F. Batyaev, Valery M. Zhivun, Evgeny I. Karpikhin, Ruslan D. Mulambetov, Dmitry V. Fischenko, Svetlana V. Kvasova - Institute for Theoretical and Experimental Physics, *B. Cheremushkinskaya 25, 117259 Moscow, Russia*
Stepan G. Mashnik, Richard E. Prael, Arnold J. Sierk Los Alamos National Laboratory,Los Alamos, NM 87545, USA

Submitted to: Proc. of the 15th Int. Workshop on Fission Physics, Obninsk, Russia, October 2-6, 2000

http://lib-www.lanl.gov/la-pubs/00393817.pdf

FISSION PRODUCT YIELDS IN HYBRID (ADS) TARGET MATERIALS INDUCED BY HIGH-ENERGY PROTONS

Yury E. Titarenko, Oleg V. Shvedov, Vyacheslav F. Batyaev, Valery M. Zhivun, Evgeny I. Karpikhin, Ruslan D. Mulambetov, Dmitry V. Fischenko, Svetlana V. Kvasova

Institute for Theoretical and Experimental Physics
B. Cheremushkinskaya 25, 117259 Moscow, Russia

Stepan G. Mashnik, Richard E. Prael, Arnold J. Sierk
Los Alamos National Laboratory,Los Alamos, NM 87545, USA

Abstract

Fission product cross sections of (p,f)-reaction in thin samples of ^{208}Pb, ^{nat}HgO, ^{nat}W irradiated with high-energy protons are measured. The irradiations were made using proton beams extracted from the ITEP synchrotron. The nuclide yields were γ-spectrometered directly using a high-resolution Ge-detector. The GENIE2000 code was used to process the measured γ-spectra and the ITEP-developed SIGMA code was used together with the PCNUDAT nuclear decay database to identify the γ-lines and to determine the cross-sections. The ^{27}Al(p,x)^{22}Na reaction was used to monitor the proton flux. The LAHET, CEM2k, CEM95, CASCADE/INPE, CASCADE, INUCL, and YIELDX codes were used for computer simulation of the products measured. Comparison of simulated and experimental values shows insufficient predictive power of the existing fission models. The results obtained are of importance in studying the parameters of the Pb, Hg and W target modules of the hybrid Accelerator-Driven System (ADS) facilities.

1. Introduction

In nucleon-irradiated heavy preactinide nuclei at energies above ~100 MeV, the fission mode (suppressed at lower energies by high fission barriers) shows itself together with the direct interaction modes. In this case, the fission fragment mass distributions are of explicit "single-hump" shape, which is what must be expected because the shell effects are insignificant at such high excitation energies of compound nuclei, and a pure drop-type fission barrier appears. A more complicated question to answer is what is the actual fissioning nucleus in this case? The fission of a compound nucleus at high energies of projectiles is preceded by at least three processes that change the nucleon balance of the reaction, namely:

(1) Intranuclear cascade emission that occur within a time comparable with the kinematic flight time of the projectile to traverse the nucleus ($\tau_0 \sim 10^{-22}$ s);

(2) Thereafter, the residual system gets thermalized within a time $\sim 5\tau_0$ and preequilibrium particles may be emitted before a proper compound nucleus is produced;

(3) Evaporation of neutrons and charged particles from the compound nucleus (a slower process, $\tau \sim 10^{-20}$s, called often pre-fission emission, which is not quite justified as this process is competing with fission).

Evaporation of particles from fission fragments ($\tau \sim 10^{-17}$s) follows the proper fission process and usually it is assumed that particle emission does not occur when the fissile system descends from the saddle point to the disruption point.

A successive superposition of the mentioned above processes together with the proper fission give rise to a very complicated nuclide composition of the reaction products. At the same time, such a composition has to be decoded in view not only to understand the phenomenon as a whole, but also to study the proper fission. According to the mentioned pattern of forming the nuclide composition of the fission fragments, the mass and charge distributions of the latter are readily seen to be extended superpositions, thus making it difficult to compare the experimental high-energy fission data with predictions by theoretical models.

In view of the above, important information may be provided by data obtained by physical and analytical methods for studying the nuclide composition of the reaction products without instrumental discrimination of the fission channel, i.e., by measuring the cross sections for production of all secondary nuclides. A joint analysis of such measurements together with data of "pure" fission experiments will make it possible to improve the consistent estimate of the reaction nuclide balance and, hence, the quality of physical interpretation of the entire set of processes discussed above.

Measurements of the produced nuclide cross sections can be made not only by a direct "physical technique", but also using "analytical methods" based on detecting and analyzing the radiation from secondary radionuclides in irradiated targets. Such analytical methods have advantages of their relative instrumental and methodological simplicities that permit large experimental data sets to be obtained within short periods of time. Besides, analytical methods provide independent verification of the physical methods and, hence, help in understanding the systematic errors inherent to both.

Among analytical methods of radionuclide analysis, the techniques of direct γ-spectrometering the irradiated target without any preliminary chemical separation are of high potential both regarding the data accumulation rate and the range of studied radionuclides. However, a successful realization of these techniques requires high-current accelerators, to provide a sufficient statistical support of measurements. The availability of such an accelerator at the Institute for Theoretical and Experimental Physics (ITEP), namely, the ITEP U-10 proton synchrotron, has made possible researches described in the present paper.

2. Experimental techniques

The experimental samples, which are 10.5-mm diameter pellets manufactured by pressing fine-dispersed powders, were irradiated together with 10.5-mm diameter Al pellets. Two independent proton beams from the ITEP U-2 synchrotron are used to irradiate the samples, namely, the low-energy (70-200 MeV) and high-energy (800-2600 MeV) beams.

Table 1 shows the composition and chemical impurity content of the experimental samples and monitors together with the main irradiation parameters and the cross section of the $^{27}Al(p,x)^{22}Na$ reaction used to monitor the protons.

After the irradiations, the γ-spectra of the samples were measured with a high energy resolution Ge-spectrometer. The yields of product nuclei were measured by the relative method using the $^{27}Al(p,x)^{22}Na$ monitor reaction cross section. The techniques for measuring γ-spectra and for determining the external proton beam energies and geometric parameters, as well as the neutron background are described in Refs. [1,2].

Table 1. Irradiation parameters, thicknesses of samples and monitors, and the $^{27}Al(p,x)^{22}Na$ monitor reaction cross sections

Sample	Isotopic composition [%]	Chemical impurity content [%]	Proton energy [GeV]	$^{27}Al(p,x)^{22}Na$ monitor reaction cross sections [mb]	Monitor sample thickness [mg/cm^2]	Proton flux through sample within irradiation time [10^{13} p/cm^2]
^{208}Pb	^{208}Pb – 97.2 ^{207}Pb - 1.93 ^{206}Pb - 0.87 ^{204}Pb - <0.01	< 0.001	1.0	15.0 ± 0.9	139.4 / 139.6	5.1
^{Nat}W	Natural	< 0.05	2.6	11.7 ± 0.9	38.1 / 139.1	5.2
^{Nat}HgO	Natural	< 0.16	0.1	19.1 ± 1.3	536.0 / 138.2	0.9
			0.2	15.1 ± 0.9	537.4 / 137.3	1.9
			0.8	15.5 ± 0.9	529.3 / 139.1	1.3
			2.6	11.7 ± 0.9	536.3 / 137.0	8.3

3. Basic definitions and computational relations

The formalism of representing the reaction product yields (cross sections) in high-energy proton-irradiated thin targets is described in sufficient detail in [1,2]. In terms of this formalism, the variations in the concentration of any two chain nuclides produced in an irradiated target ($N_1 \xrightarrow{\lambda_1} N_2 \xrightarrow{\lambda_2}$) may be presented to be a set of differential equations that describe the production and decays of the nuclides. By introducing a formal representation of the time functions of the type $F_i(t)=\left(1-e^{-\lambda_i\tau}\right)\cdot\frac{1-e^{-\lambda_i kT}}{1-e^{-\lambda_i T}}$ (i =*1, 2, or Na*; τ is the duration of a single proton pulse; T is pulse repetition period; k is the number of pulses within the irradiation period), which characterize the nuclide decays within the irradiation time, and by expressing (similar to the relative measurements) the proton fluence via the monitor reaction cross section σ_{st}, we can present the unknowns as

$$\sigma_1^{cum}=\frac{A_0}{\eta_1\varepsilon_1F_1N_{Na}}\cdot\frac{N_{Al}}{N_T}\cdot\frac{F_{Na}}{\lambda_{Na}}\cdot\sigma_{st} \quad (1)$$

$$\sigma_1^{cum}=\frac{A_1}{\nu_1\eta_2\varepsilon_2F_1N_{Na}}\cdot\frac{N_{Al}}{N_T}\cdot\frac{\lambda_2-\lambda_1}{\lambda_2}\frac{F_{Na}}{\lambda_{Na}}\cdot\sigma_{st} \quad (2)$$

$$\sigma_2^{ind}=\left(\frac{A_2}{F_2}+\frac{A_1}{F_1}\cdot\frac{\lambda_1}{\lambda_2}\right)\cdot\frac{1}{\eta_2\varepsilon_2N_{Na}}\cdot\frac{N_{Al}}{N_T}\cdot\frac{F_{Na}}{\lambda_{Na}}\cdot\sigma_{st} \quad (3)$$

$$\sigma_2^{cum}=\sigma_2^{ind}+\nu_1\cdot\sigma_1^{cum}=\left(\frac{A_1}{F_1}+\frac{A_2}{F_2}\right)\cdot\frac{1}{\eta_2\varepsilon_2N_{Na}}\cdot\frac{N_{Al}}{N_T}\cdot\frac{F_{Na}}{\lambda_{Na}}\cdot\sigma_{st} \quad . \quad (4)$$

Here, σ_1^{cum} is the cumulative cross section of the first nuclide; σ_2^{ind} and σ_2^{cum} are the independent and cumulative cross sections of the second nuclide; N_{Al} and N_T are the numbers of nuclei in the monitor and in the experimental sample, respectively; η_1 and η_2 are γ-line yields; ε_1 and ε_2 are the spectrometer efficiency at energies E_1 and E_2; ν_1 is the branching ratio of the first nuclide; λ_1, λ_2, λ_{Na} are, respectively, the decay constants of the first and second nuclides and of the monitor (^{22}Na or ^{24}Na).

The factors A_0,, A_1, and A_2 are calculated through fitting the measured counting rates in the total absorption peaks, which correspond to energies E_1 (the first nuclide) and E_2 (the second nuclide), by exponential functions. It should be noted that formulas (1)-(4) were deduced on the assumption that the γ-intensities of the two nuclides produced under irradiation are recorded up to the desired accuracy within a period from irradiation end to the moment of the ultimate detectable intensity. If, for some reasons, the factor A_1 cannot be found, then the factor A_2 will be used together with expression (14) from [1] to determine the constant (σ_2^{cum*}), which we called the supra cumulative yield:

$$\sigma_2^{cum^*} = \sigma^{ind}{}_2 + \frac{\lambda_1}{\lambda_1 - \lambda_2} \nu_1 \cdot \sigma_1^{cum} = \frac{A_2}{N_T \Phi \eta_2 \varepsilon_2 F_2} \qquad (5)$$

The resultant value may prove to be very different from σ_2^{cum}. Nevertheless, the supra cumulative yield can be either used directly to verify the codes, or determined further up to σ_2^{cum} if the necessary cross section is obtained elsewhere (for example in the "inverse" kinematics experiments).

4. Experimental results

In our experiments, 596 yields of residual product nuclei were determined, of which more than a hundred yields are fission products (see Table 2). It should be noted that the present experimental data are slightly different from the preliminary results reported earlier [18,19], as our data acquisition is persistently in progress.

Table 2. Statistics of the product nuclei obtained in the experiments

Target	Energy [GeV]	Number of the product nuclei measured						
		I	Σm_j	Σm_j+g	C	C*	Sub-total	of them, fission products
^{208}Pb	1.0	8	15	15	65	11	114	30
^{Nat}W	2.6	10	9	6	100	4	129	17
^{Nat}Hg	0.1	4	10	12	17	1	44	8
	0.2	6	12	14	27	6	65	13
	0.8	9	12	14	57	11	103	21
	2.6	8	16	14	90	13	141	30
						TOTAL	**596**	**119**

Legend:
I - independent yields
Σm_j – independent yields of separate metastable states
Σm_j+g – independent yields of metastable and ground states
C – cumulative yields
C* - supra cumulative yields

It should be noted that the number of the measured fission products were counted on the assumption that a measured nuclide is considered as a fission product for mass numbers below or equal to 121 for ^{208}Pb, 97 for ^{nat}W, 111 for ^{nat}Hg at 0.1 GeV, 0.2 GeV, and 0.8 GeV, and 103 for ^{nat}Hg at 2.6 GeV.

5. Simulation of experimental results

Simulation techniques are of essential importance when forming a set of nuclear constants to be used in designing ADS facilities because they are universal and save much time and labour. At the same time, the present-day accuracy and reliability of the simulated data are inferior to experiment. Also existing simulation codes have different predictive abilities when used to study the reactions that are of practical importance.

Considering this, the present work is aimed also at verifying the simulation codes used most extensively for this purpose in order to estimate their predictive abilities and to stimulate efforts to improve them.

The following seven simulation codes were examined to meet these requirements:

- the CEM95 cascade-exciton model code [3],
- the CASCADE cascade-evaporation-fission-transport code [4],
- the INUCL cascade- preequilibrium-evaporation-fission code [5],
- the LAHET cascade-preequilibrium-evaporation-fission code (ISABEL option) [6],
- the YIELDX semi-phenomenological code [7],
- the CASCADE/INPE cascade-preequilibrium-evaporation-fission-transport code [8],
- the latest version of the improved cascade-exciton model [9] code, CEM2k [10].

All the above codes are described in detail in [1,2,10,11].

Contrary to the simulation results, the experimental data include not only independent, but also (and mainly) cumulative and supra cumulative residual product nuclei. To get a correct comparison between the experimental and simulation data, the cumulative yields must be calculated on the basis of the simulated independent yields.

Since any branched isobaric chain can be presented to be a superposition of a few linear chains, the theoretical cumulative and supra cumulative yields of the *n*-th nuclide can be calculated as

$$\sigma_n^{cum} = \sigma_n^{ind} + \sum_{i=1}^{n-1} \sigma_i^{ind} \prod_{j=i}^{n-1} \nu_j \,, \tag{6}$$

$$\sigma_n^{cum^*} = \sigma_n^{ind} + \frac{\lambda_{n-1}}{\lambda_{n-1} - \lambda_{n1}} \nu_{n-1} \sigma_{n-1}^{ind} + \sum_{i=1}^{n-2} \left(\sigma_i^{ind} \prod_{i=1}^{n-2} \nu_j \right) \tag{7}$$

To get a correct comparison between results obtained by different codes, the calculations were renormalized to the same cross sections for proton-nucleus inelastic interactions [12].

If an experiment-simulation difference of no more than 30% ($0.77<\sigma_{calc.}/\sigma_{exp.}<1.3$) is taken to be the coincidence criterion [13], the simulation accuracy can be defined as the ratio of the number of such coincidences to the number of the comparison events. The 30% level meets the accuracy requirements of cross sections for nuclide production to be used in designing ADS plants, according to [13]. The mean simulated-to-experimental data ratio can be used as another coincidence criterion [1]:

$$\langle F \rangle = 10^a \,, \quad \text{where} \quad a = \sqrt{\left\langle \left(\log(\sigma_{cal,i} / \sigma_{\exp,i} \right)^2 \right\rangle} \,, \tag{8}$$

with its standard deviation

$$S(\langle F \rangle) = \left\langle \left(\left| \log\left(\sigma_{calc,i} / \sigma_{\exp,i}\right) \right| - \log\left(\langle F \rangle\right) \right)^2 \right\rangle \,, \tag{9}$$

where $\langle\ \rangle$ designates averaging over all the experimental and simulated results used in the comparison ($i = 1, \ldots, N_S$).

The mean ratio <F>, together with its standard deviation S(<F>) defines the interval [⟨F⟩/S(⟨F⟩) , ⟨F⟩*S(⟨F⟩)] that covers about 2/3 of the simulation-to-experiment ratios.

We apply the above two criteria together with our results shown in Figs. 1-14, to infer conclusions about the predictive power of a given code.

The default options were used in all of the simulation codes without modifying the codes to get optimal agreement with the data. All the calculations were made before any experimental results were obtained, except the results from CEM2k. With such an approach, our comparison demonstrate the real predictive power, rather than the descriptive power of the codes.

6. Comparison of experiment with simulations

The results obtained with the codes are presented in

- Figs. 1 through 6, which show the results of a detailed comparison between the simulated and experimental data on the radioactive reaction product yields;
- Figs. 7 through 12, which show the simulated mass distributions of the reaction products together with the measured cumulative and supra cumulative yields of the products that are in immediate proximity to the stable isobar of a given mass (the sum of such yields from either sides in cases when both left- and right-hand branches of the chain are present). Obviously, the simulation results do not contradict the experimental data if calculated values run above the experimental data and follow a general trend of the latter. This is because direct γ-spectroscopy identifies only the radioactive products, which generally form a significant fraction of the total mass yield but are never equal to the total mass yield when a stable isobar is produced;
- Fig. 13, which shows the experimental and calculated yields for several nuclides from Hg versus the proton incident energy;
- Fig. 14, which shows our [2] and GSI [14] experimental data and simulated independent yields of Tm, Ir, and Tl isotopes from ^{208}Pb in the form of isotopic mass distributions.

Table 3 presents the statistics of the experimental-to-simulated reaction product yield comparisons for the spallation and fission reactions separately, namely: the total number of measured yields, N_T; the number of the measured yields selected to compare with simulated data, N_G; the number of the product nuclei whose yields were simulated by a particular code, N_S**;** the number of the comparison events when the simulated data differ from the experimental results by not more than 30%, $N_{C1.3}$; and the number of the comparison events when the simulated data differ from the experimental results by not more than a factor of 2.0, $N_{C2.0}$.

Generally, for each reaction studied here there is a region of products where both deep spallation and fission mechanisms are involved, i.e., the net measured yield of nuclides in this "overlapping" region contains contributions both from spallation and fission. To have a "pure" comparison with the data of calculated spallation and fission fragment yields, we do exclude from our comparisons shown in Tab. 3 the products from the "overlapping" regions. For each reaction, the overlapping region is different and we estimated it comparing the measured data points with calculations by LAHET and other codes, where each nuclide produced has an explicit index, either it is a spallation or a fission product, so that we get separately contributions from both spallation and fission to the total calculated yield. We "defined" the overlapping regions following: 120<A<153 for ^{208}Pb at

1 GeV, 84<A<99 for ^{nat}W at 2.6 GeV, 95<A<121 for ^{nat}Hg at 2.6 GeV, and 105<A<160 for ^{nat}Hg at 800 MeV (no measured yields in the overlapping regions for ^{nat}Hg at 200 and 100 MeV). Nuclides from these overlapping regions are excluded from comparisons shown in columns "spallation" and "fission" of Tab. 3, but are includes in its last column and in Figs. 1-6, where comparisons for all measured yields are shown.

Since about a third of all secondary nuclei from our reactions are not spallation products, the ability of codes to simulate high-energy fission processes is an important criterion of their ability to work when the target is heavy enough to fission.

Among the code used here, LAHET, CASCADE, INUCL, CASCADE/INPE, and YIELDX simulate both spallation and fission products. The CEM2k and CEM95 codes simulate spallation only and do not calculate the process of fission, and do not provide fission fragments an a further possible evaporation of particles from them. When, during a Monte-Carlo simulation of the compound stage of a reaction these code encounter a fission, they simply remember this event (that permit them to calculate fission cross section and fissility) and finish the calculation of this event without a subsequent calculation of fission fragments. Therefore, results from CEM2k and CEM95 shown here reflect the contribution to the total yields of the nuclides only from deep spallation processes of successive emission of particles from the target, but do not contain fission products. This is explicitly reflected in a smaller number of the products simulated (the quantity Ns in Table 3) and the shapes of the simulated curves in Figs. 1-12. To be able to describe nuclide production in the fission region, these codes have to be extended by incorporating a model of high energy fission (e.g., in the transport code MCNPX [15], where CEM97 [9] is used, it is supplemented by the RAL fission model [16]).

The following conclusions follow from the analysis of the results for ^{208} Pb and ^{nat}W presented in Table 3 and in Figs. 1, 2, 7, 8, and 14:

1. Generally, all the codes can reasonably simulate the weak spallation reactions (the A ≥180 products for ^{208}Pb and the A ≥150 products for ^{nat}W), with simulation results differing from experimental data, usually within a factor of 2.
2. In the deep spallation range (150<A<180 for ^{208}Pb and 110<A<150 for ^{nat}W) the simulation codes have very different predictive powers, namely,
   - the LAHET, CEM2k, CASCADE/INPE, and YIELDX predictions are very close to the experimental data;
   - on the whole, the CASCADE code simulates the A>160 product yields adequately. Below A = 160, however, the simulated results are underestimated progressively (up to a factor of 5);
   - the INUCL code underestimates all the product yields systematically by a factor of 2-10 with the discrepancy increasing with decreasing A.
3. In the range of fission products (50<A<150 for ^{208}Pb and 30<A<110 for ^{nat}W), the INUCL code predictions are in the best agreement with the data, when describing the yields from ^{208}Pb. As a rule, the INUCL-simulated yields differ from measured data by a factor of less than 1.5. In the case of ^{nat}W, however, the prediction quality deteriorates substantially. The LAHET-simulated yields in the same mass range are underestimated by a factor of 1.5-10.0. The specific predictions of isotope production cross sections of the semi-phenomenological code YIELDX both under- and over-estimate the fission product data by a factor of up to 30, without showing any obvious patterns in disagreement (Figs. 1-6). In contrast, the YIELDX isobar cross sections are all greatly overpredicted, as shown in Figs. 7, 8, 10, 11, and 12.

Table 3. Statistics of the experimental-to-simulated spallation and fission yield comparisons

Code	Spallation			Fission			All products (spallation+fission+ fragmentation)		
^{208}Pb	N_T = 74, N_G = 55			N_T = 30, N_G = 15			N_T = 114, N_G = 76		
E_p=1.0GeV	$N_{C1.3}$ / $N_{C2.0}$ / N_S	⟨F⟩	S(⟨F⟩)	$N_{C1.3}$ / $N_{C2.0}$ / N_S	⟨F⟩	S(⟨F⟩)	$N_{C1.3}$ / $N_{C2.0}$ / N_S	⟨F⟩	S(⟨F⟩)
LAHET	36/51/55	1.39	1.31	1/3/15	3.65	1.70	39/59/76	1.92	1.73
CEM2k	33/53/55	1.40	1.25	--	--	--	33/54/60	1.62	1.45
CASCADE/INPE	26/47/51	1.52	1.34	4/9/15	2.24	1.70	32/56/70	1.85	1.59
CASCADE	24/46/54	1.61	1.37	5/9/15	2.59	1.94	29/55/72	2.18	1.88
YIELDX	23/42/55	1.82	1.53	1/3/15	7.04	2.57	27/49/76	2.76	2.24
CEM95	30/46/55	2.16	2.00	--	--	--	30/46/55	2.16	2.00
INUCL	16/27/55	2.75	1.99	7/11/14	1.95	1.71	24/40/73	2.89	2.15
^{Nat}W	N_T = 100, N_G = 61			N_T = 17, N_G = 14			N_T = 129, N_G = 81		
E_p=2.6GeV	$N_{C1.3}$ / $N_{C2.0}$ / N_S	⟨F⟩	S(⟨F⟩)	$N_{C1.3}$ / $N_{C2.0}$ / N_S	⟨F⟩	S(⟨F⟩)	$N_{C1.3}$ / $N_{C2.0}$ / N_S	⟨F⟩	S(⟨F⟩)
CEM95	31/56/61	1.53	1.36	--	--	--	31/57/69	2.40	2.20
CASCADE	37/54/61	1.54	1.42	2/4/13	5.43	3.12	39/61/79	2.26	2.07
CEM2k	18/51/61	1.71	1.34	--	--	--	19/55/71	2.10	1.65
LAHET	11/49/61	1.81	1.35	0/3/11	6.36	2.97	11/53/77	2.51	1.90
YIELDX	22/40/61	1.88	1.47	3/8/14	2.30	1.70	25/51/81	2.04	1.56
INUCL	28/49/61	2.06	1.82	0/0/5	14.16	1.86	28/49/70	3.43	2.88
^{Nat}Hg	N_T = 36, N_G = 24			N_T = 8, N_G = 5			N_T = 44, N_G = 29		
E_p=0.1GeV	$N_{C1.3}$ / $N_{C2.0}$ / N_S	⟨F⟩	S(⟨F⟩)	$N_{C1.3}$ / $N_{C2.0}$ / N_S	⟨F⟩	S(⟨F⟩)	$N_{C1.3}$ / $N_{C2.0}$ / N_S	⟨F⟩	S(⟨F⟩)
CEM2k	6/18/23	1.73	1.36	--	--	--	6/18/23	1.73	1.36
LAHET	8/16/23	1.78	1.43	0/0/3	7.88	1.45	8/16/26	2.43	1.92
INUCL	8/15/23	2.12	1.64	0/0/4	6.97	1.77	8/15/27	2.77	2.02
CASCADE	12/16/23	2.15	1.88	0/2/4	3.77	2.07	12/18/27	2.39	1.99
CEM95	8/14/24	2.19	1.68	--	--	--	8/14/24	2.19	1.68
^{Nat}Hg	N_T = 52, N_G = 35			N_T = 13, N_G = 7			N_T = 65, N_G = 42		
E_p=0.2GeV	$N_{C1.3}$ / $N_{C2.0}$ / N_S	⟨F⟩	S(⟨F⟩)	$N_{C1.3}$ / $N_{C2.0}$ / N_S	⟨F⟩	S(⟨F⟩)	$N_{C1.3}$ / $N_{C2.0}$ / N_S	⟨F⟩	S(⟨F⟩)
LAHET	17/30/35	1.50	1.30	0/1/6	3.70	1.74	17/31/41	1.87	1.60
CEM2k	20/29/35	1.59	1.41	--	--	--	20/29/35	1.59	1.41
YIELDX	15/31/35	1.59	1.33	0/3/7	2.55	1.47	15/34/42	1.77	1.43
CASCADE	10/28/35	2.09	1.75	2/3/6	3.36	2.26	12/31/41	2.28	1.87
CEM95	12/28/35	2.13	1.84	--	--	--	12/28/35	2.13	1.84
INUCL	10/21/35	2.22	1.69	2/2/6	2.66	1.77	12/23/41	2.29	1.71
^{Nat}Hg	N_T = 66, N_G = 47			N_T = 21, N_G = 13			N_T = 103, N_G = 70		
E_p=0.8GeV	$N_{C1.3}$ / $N_{C2.0}$ / N_S	⟨F⟩	S(⟨F⟩)	$N_{C1.3}$ / $N_{C2.0}$ / N_S	⟨F⟩	S(⟨F⟩)	$N_{C1.3}$ / $N_{C2.0}$ / N_S	⟨F⟩	S(⟨F⟩)
CASCADE	26/43/46	1.43	1.26	4/7/12	2.49	1.85	31/51/66	2.33	2.08
LAHET	31/44/47	1.45	1.32	1/1/12	3.97	1.58	36/54/69	1.96	1.71
CEM2k	23/45/47	1.45	1.26	--	--	--	24/47/54	1.73	1.51
CEM95	33/44/47	1.54	1.50	--	--	--	33/44/51	2.30	2.28
YIELDX	18/37/47	1.68	1.36	4/5/13	3.29	2.08	27/51/70	2.09	1.72
INUCL	22/34/46	1.88	1.57	2/3/11	4.36	2.28	24/37/65	2.68	2.02
^{Nat}Hg	N_T = 92, N_G = 61			N_T = 30, N_G = 21			N_T = 141, N_G = 90		
E_p=2.6GeV	$N_{C1.3}$ / $N_{C2.0}$ / N_S	⟨F⟩	S(⟨F⟩)	$N_{C1.3}$ / $N_{C2.0}$ / N_S	⟨F⟩	S(⟨F⟩)	$N_{C1.3}$ / $N_{C2.0}$ / N_S	⟨F⟩	S(⟨F⟩)
CASCADE	38/56/61	1.50	1.37	5/11/17	2.04	1.49	44/73/86	1.64	1.44
CEM95	36/56/61	1.52	1.38	--	--	--	37/59/68	1.88	1.74
LAHET	12/49/60	1.73	1.26	5/10/19	2.63	1.87	17/63/87	2.00	1.48
CEM2k	17/51/61	1.73	1.36	--	--	--	22/58/73	2.40	2.03
INUCL	21/50/61	1.87	1.58	4/9/16	2.85	2.04	26/61/85	2.43	1.97
YIELDX	15/45/61	2.01	1.55	3/7/20	3.65	1.98	19/55/89	2.45	1.76

The CASCADE/INPE-simulated yields of the 130<A<150 reaction products are strongly underestimated (up to 1-2 orders of magnitude), while the rest of the simulated fission product yields (40<A<130) agree with the experimental data generally within a factor of 2. Generally, all the codes exhibit the feature noted above for INUCL, namely, the prediction quality in the case of ^{nat}W is much worse compared to ^{208}Pb, probably, because the cross section for fission of a compound nucleus of a very low fissility is especially difficult to calculate.

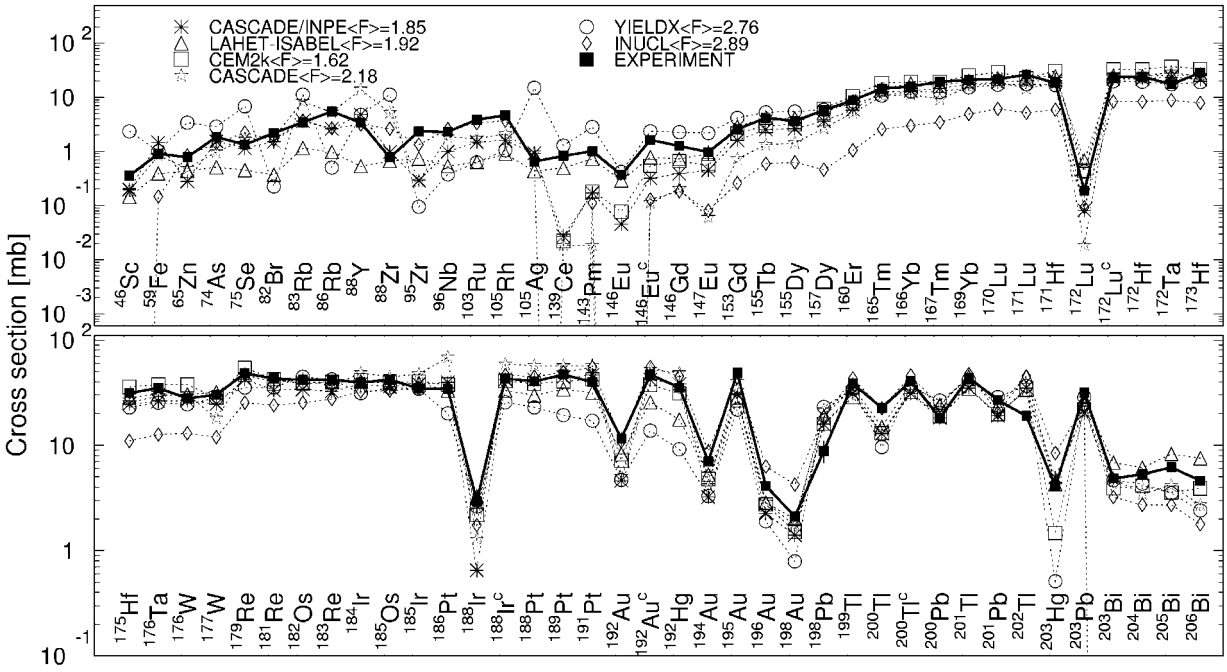

Fig. 1. Product-by-product comparison between the experimental and simulated yields of radioactive reaction products from ^{208}Pb bombarded with 1 GeV protons.

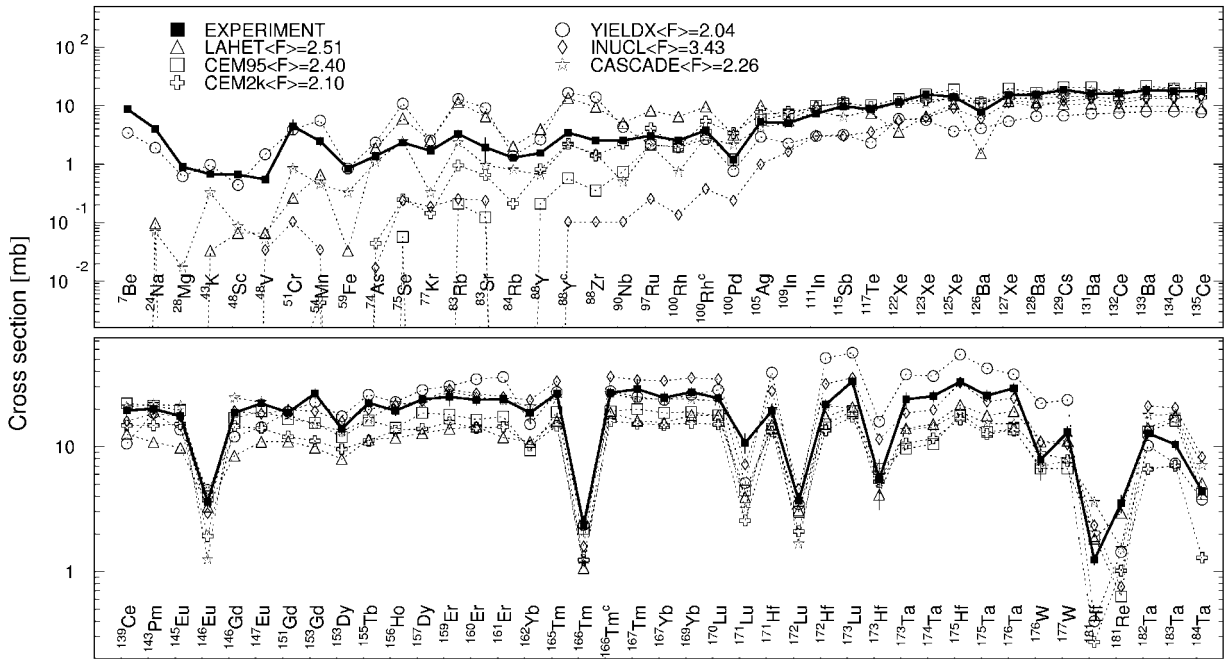

Fig. 2. Product-by-product comparison between the experimental and simulated yields of radioactive reaction products from ^{nat}W bombarded with 2.6 GeV protons.

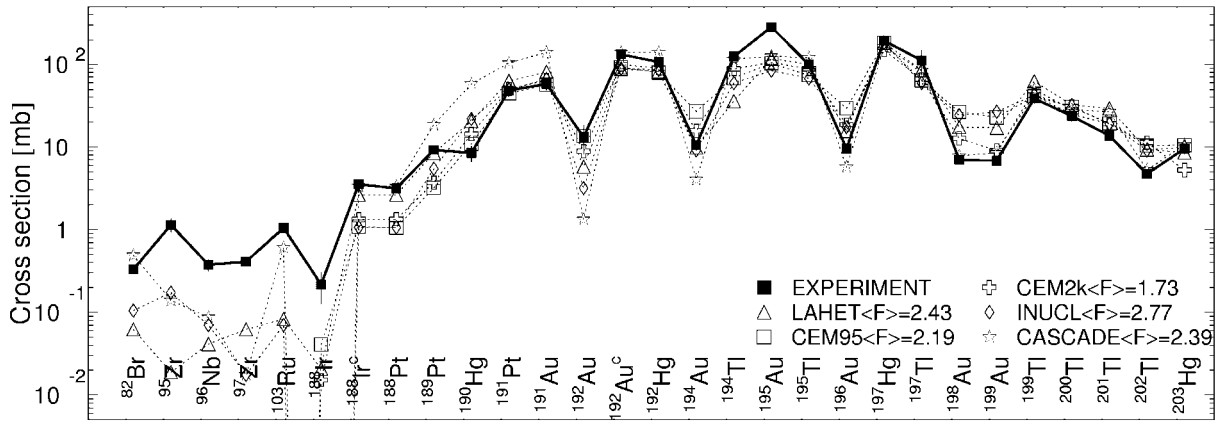

Fig. 3. Product-by-product comparison between the experimental and simulated yields of radioactive reaction products from ^{nat}Hg bombarded with 0.1 GeV protons.

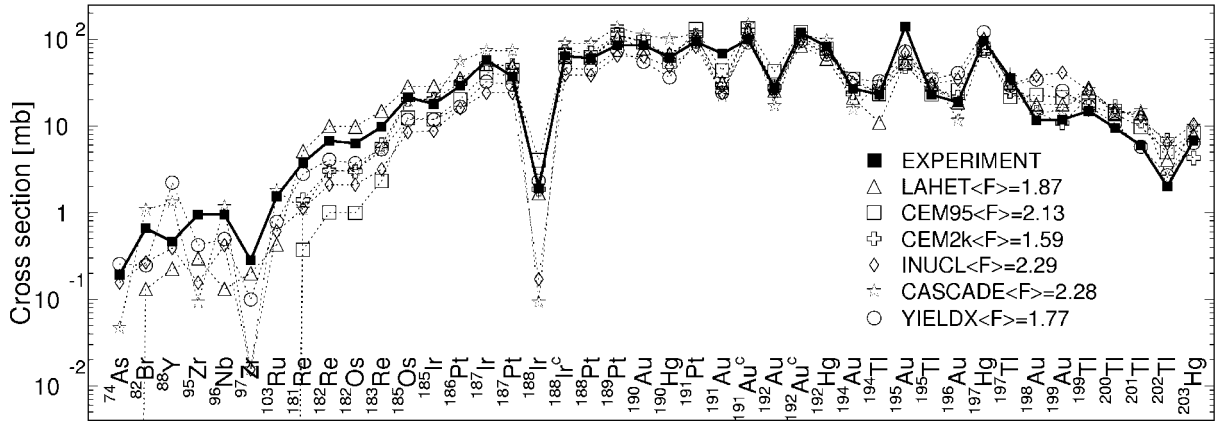

Fig. 4. Product-by-product comparison between the experimental and simulated yields of radioactive reaction products from ^{nat}Hg bombarded with 0.2 GeV protons.

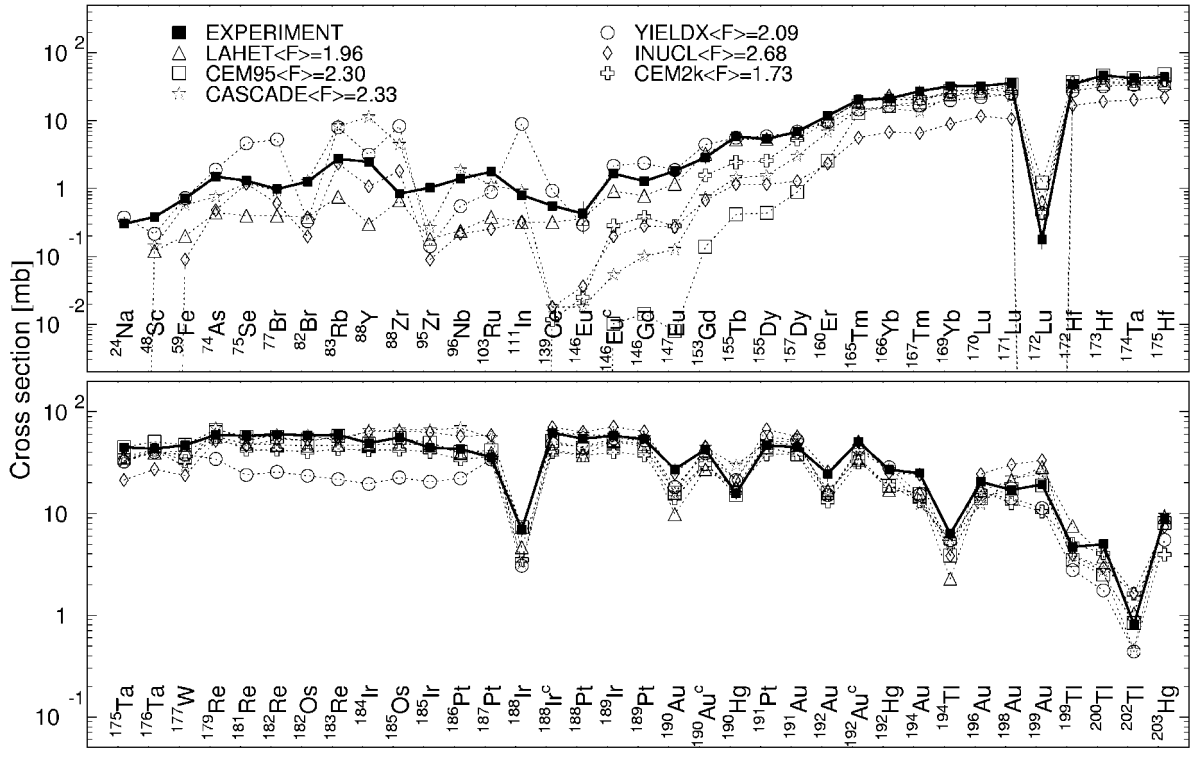

Fig. 5. Product-by-product comparison between the experimental and simulated yields of radioactive reaction products from ^{nat}Hg bombarded with 0.8 GeV protons.

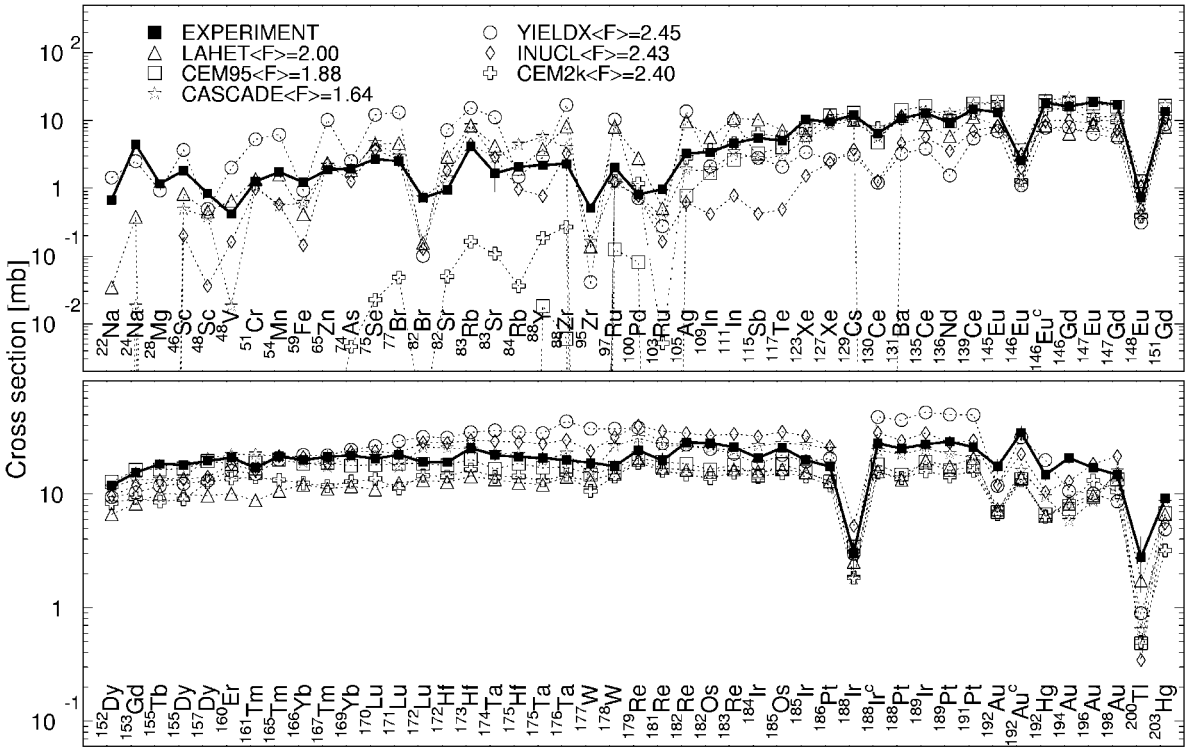

Fig. 6. Product-by-product comparison between the experimental and simulated yields of radioactive reaction products from ^{nat}Hg bombarded with 2.6 GeV protons.

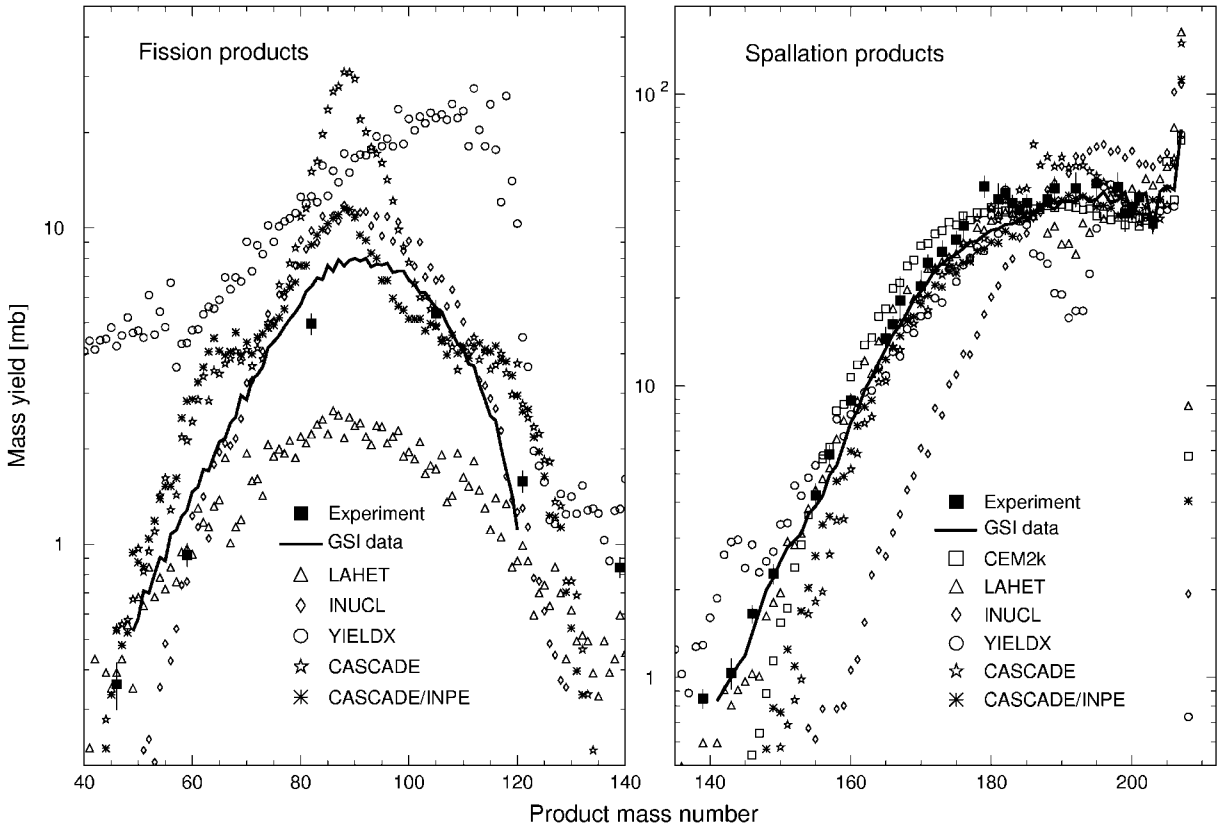

Fig. 7. The simulated mass distributions of reaction products together with the measured cumulative and supra-cumulative yields from ^{208}Pb bombarded with 1 GeV protons. Black line shows the GSI data in reverse kinematics [14].

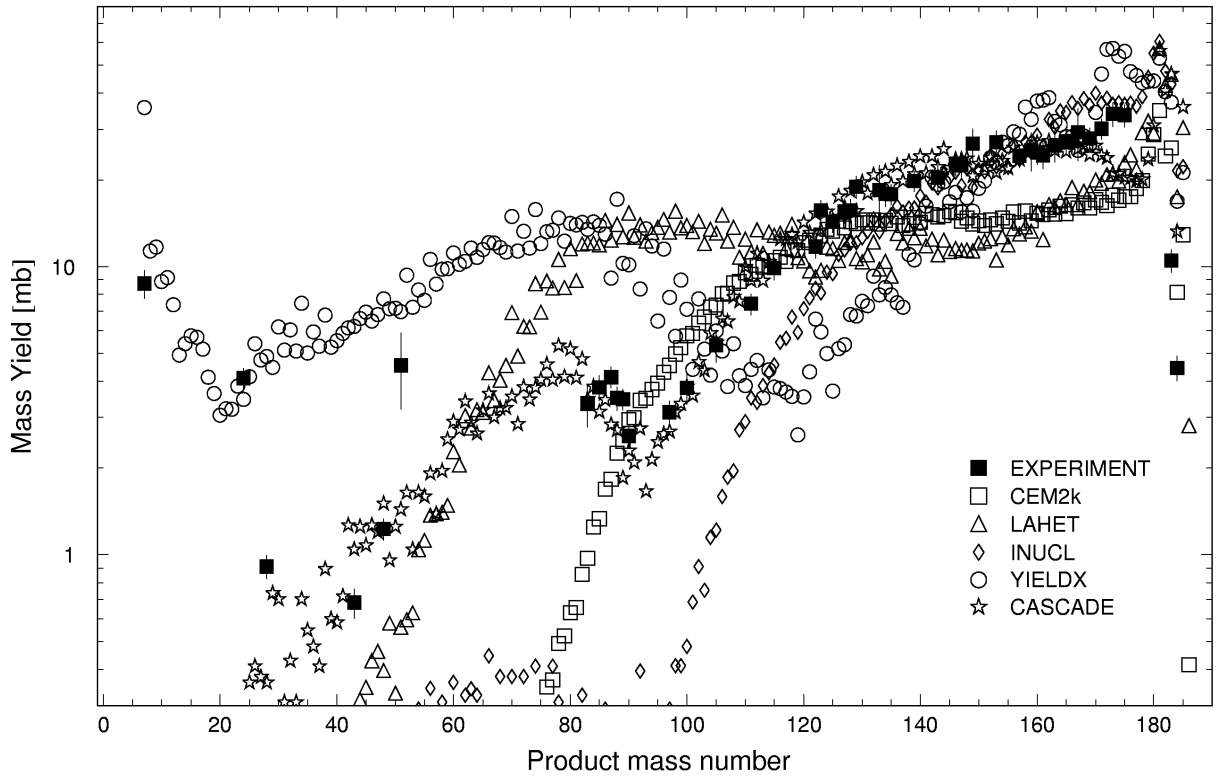

Fig. 8. The simulated mass distributions of reaction products together with the measured cumulative and supra-cumulative yields from ^{nat}W bombarded with 2.6 GeV protons.

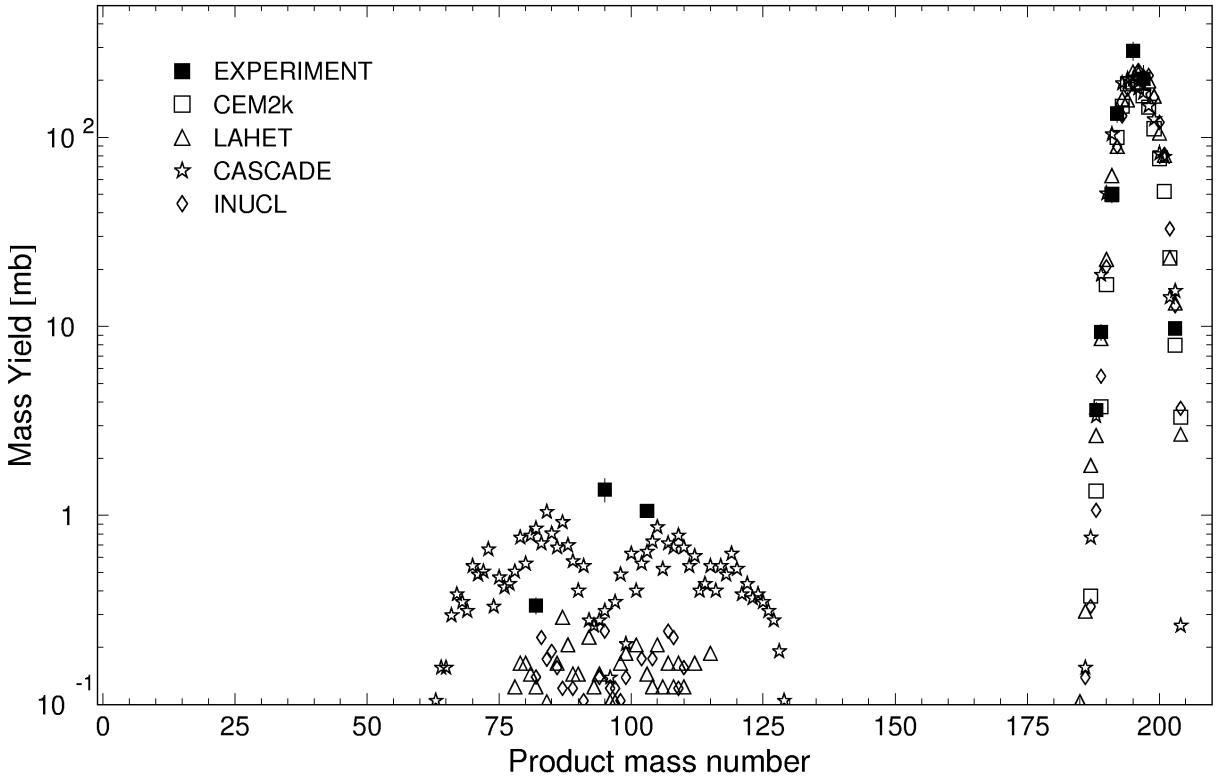

Fig. 9. The simulated mass distributions of reaction products together with the measured cumulative and supra-cumulative yields from ^{nat}Hg bombarded with 0.1 GeV protons.

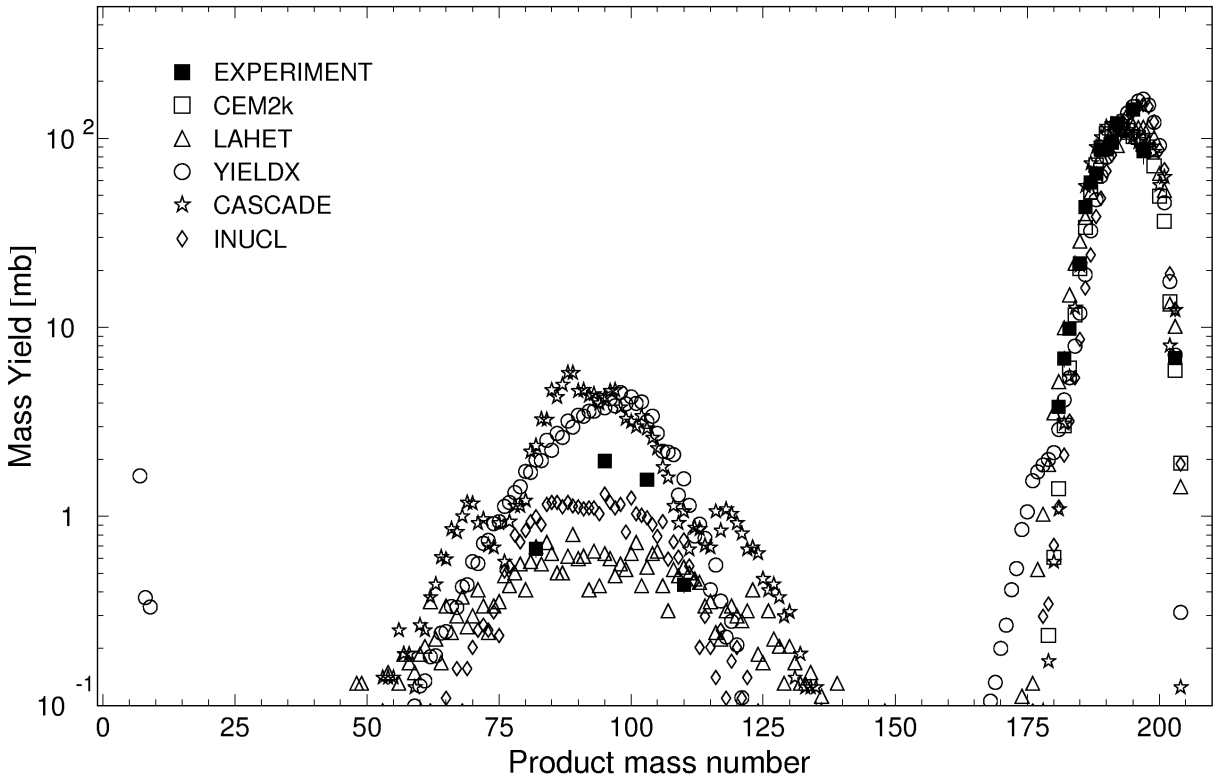

Fig. 10. The simulated mass distributions of reaction products together with the measured cumulative and supra-cumulative yields from ^{nat}Hg bombarded with 0.2 GeV protons.

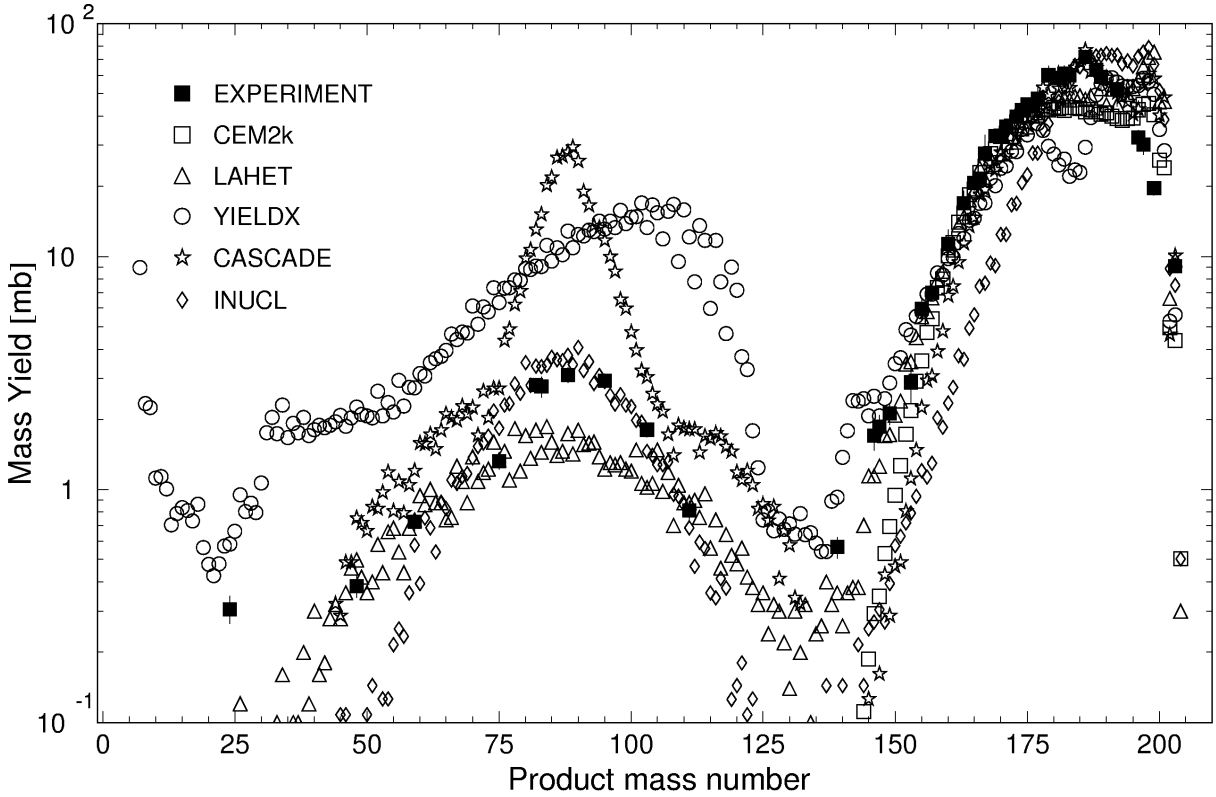

Fig. 11. The simulated mass distributions of reaction products together with the measured cumulative and supra-cumulative yields from ^{nat}Hg bombarded with 0.8 GeV protons.

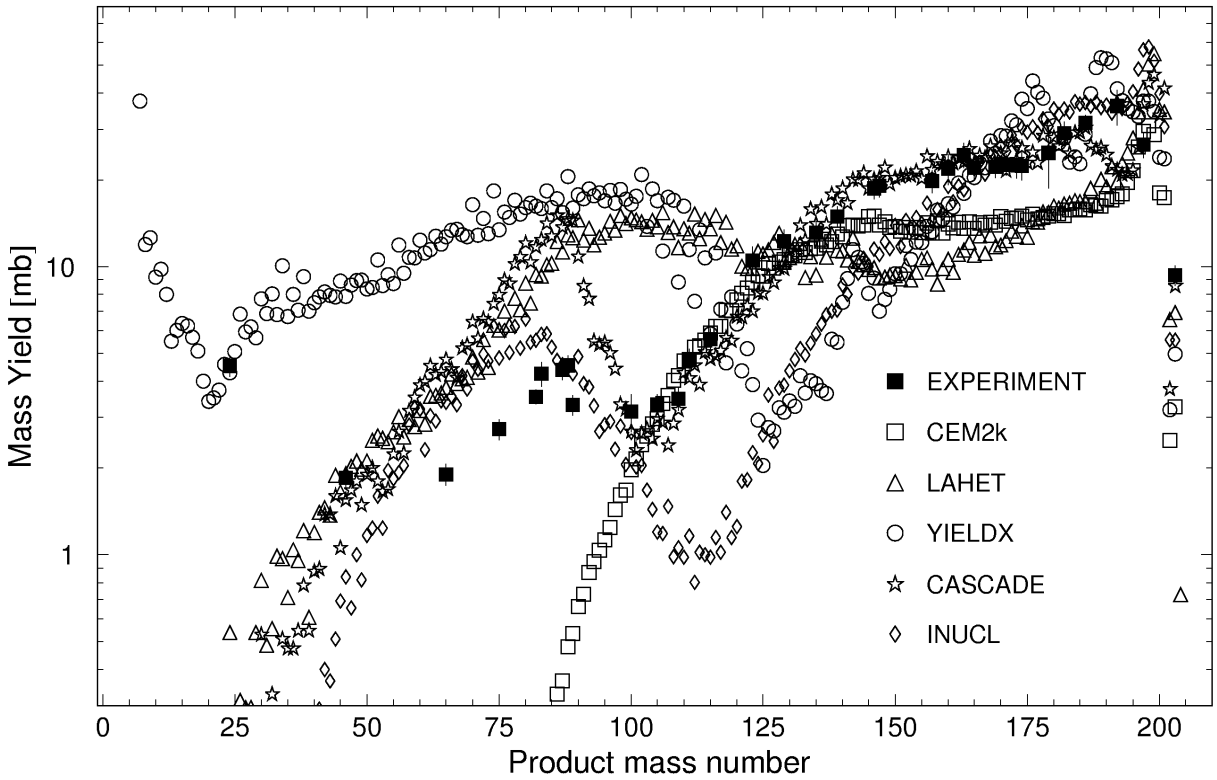

Fig. 12. The simulated mass distributions of reaction products together with the measured cumulative and supra-cumulative yields from ^{nat}Hg bombarded with 2.6 GeV protons.

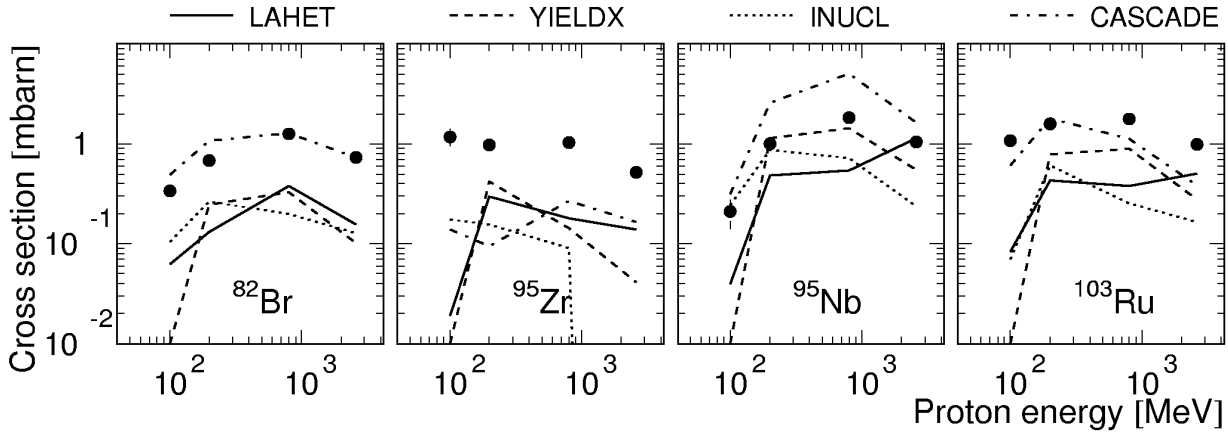

Fig. 13. Yields of indicated nuclides from ^{nat}Hg versus the incident proton energy.

In addition, the agreement of all codes with the data in the fission product region is worse than in the spallation region; therefore, development of a better model for fission-fragment formation is welcomed for any code

A comparison between the experimental and simulated data on the reaction product yields from ^{nat}Hg presented in Table 3 and in Figs. 3-6 and 9-13 shows that all codes (except for YIELDX) satisfactorily predict the A>170 products for 0.1, 0.2, and 0.8 GeV protons and the A>120 product yields for 2.6 GeV protons. The yields simulated by all codes in the remaining ranges of masses are very different from measured data, with the largest differences in the 80<A<103 range for the 0.1 and 0.2 GeV protons, in the 48<A<130 range for the 0.8 GeV protons, and in the 28<A<100 range for the 2.6 GeV protons.

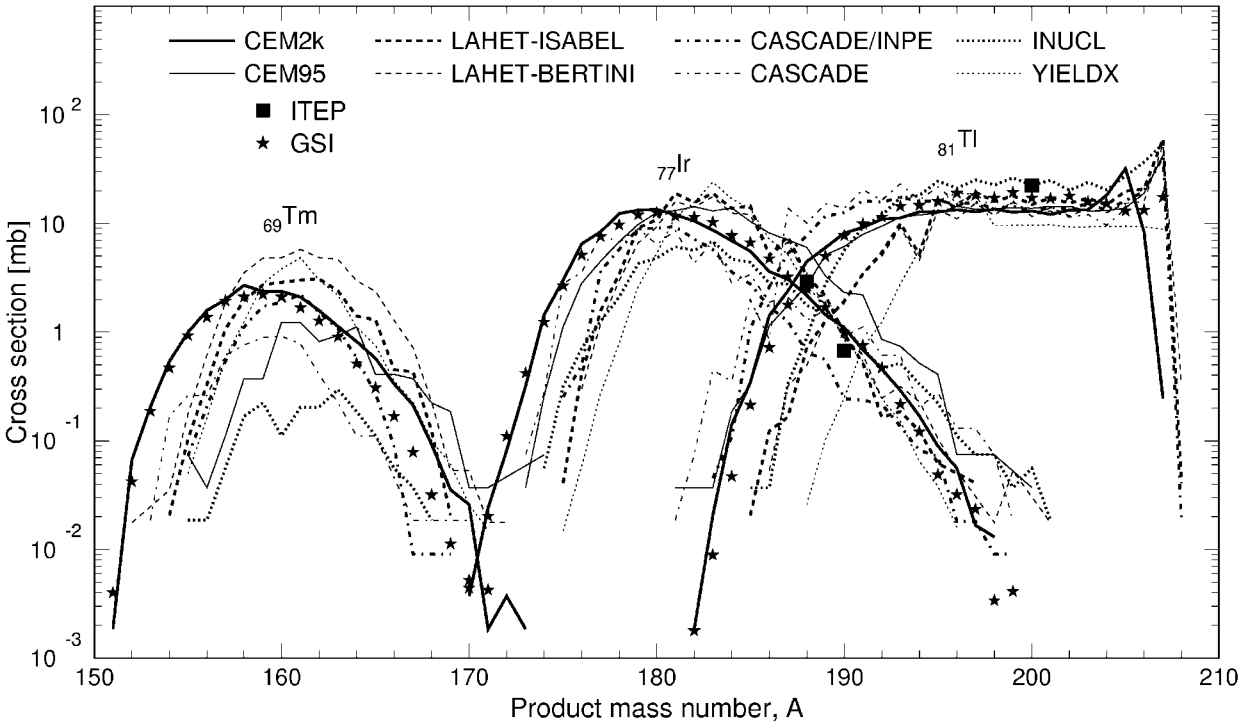

Fig. 14. Isotope mass distribution for independent production of Tm, Ir, and Tl isotopes from ^{208}Pb. Black squares are our measurements [2], while filled stars show GSI data obtained in reverse kinematics [14]. Results from different codes are marked as indicated.

Figs. 9-12 show the simulated mass yield of the reaction products. The experimental cumulative yields, which are often almost equal to the mass yields within measurement errors, are shown as well for comparison. The following conclusions may be drawn from a comparison between the experimental and simulated mass yields:

- in the case of 0.1 GeV protons and A>190, all codes[1] predict the mass curve shape quite well;
- in the case of 0.2 GeV protons and A>180, all simulated yields are in a good agreement with experiment, for all codes;
- in the case of 0.8 GeV protons, the best agreement with the data is reached with YIELDX at A>130 and with INUCL at A<130;
- in the case of 2.6 GeV protons and A>100, the CEM95 and CASCADE results agree with experiment, while the LAHET-simulated yields are underestimated, whereas the YIELDX and INUCL code-simulated yields represent the mass curve shape erroneously. None of the codes can represent the experimental curve shape at A<100.

Fig. 13 illustrates the dependence of a part of measured yields from Hg as functions of the incident proton energy together with the results by LAHET, YIELDX, INUCL, and CASCADE.

7. Conclusion

The above-presented experimental data (our data acquisition is persistently in progress) can be used to estimate the prediction power of codes and, hence, make it possible to improve the physical models used to describe reactions in heavy pre-actinide nuclei.

[1] Except for YIELDX, which was not used at 0.1 GeV.

Our study shows that the predictive power of all codes tested here for data in the fission region is worse than in the spallation region; therefore, development of better models for fission-fragment formation is of first priority. We conclude that none of the above-discussed codes can adequately describe the nuclide composition of the high-energy fission products (as a rule, a mean squared deviation factor of 2-6 is observed contrary to 1.4-2.5 for the spallation products). All tested codes should be improved further to become reliable tools for both scientific and applied purposes. We plan to test in the future one more code, namely, CEF, taking into account its potential in describing the fission processes, as reported in [17].

Further accumulation of similar experimental data is important. It should be emphasized that the charge distributions in the isobaric decay chains are important as well. The information thus obtained would make it possible, first, to raise the information content of the comparisons between experimental and simulated data and, second, to reduce the uncertainties in experimental determination of the cumulative yields by establishing unambiguous relations between σ^{cum} and σ^{cum*} for many of the reaction products.

Acknowledgments

We are indebted to Drs. T. Enqvist and B. Mustapha for providing us the cross sections measured at the GSI, to Dr. F. E. Chukreev for helpful comments on the nuclear-chain data, and to Prof. V. Artisyuk for useful discussions and help.

The work has been performed under the ISTC Project #839 supported by the European Community, Japan (JAERI), and Norway and was partially supported by the U. S. Department of Energy.

References

[1] Yu. E. Titarenko, O. V. Shvedov, M. M. Igumnov, S. G. Mashnik, E. I. Karpikhin, V. D. Kazaritsky, V. F. Batyaev, A. B. Koldobsky, V. M. Zhivun, A. N. Sosnin, R. E. Prael, M. B. Chadwick, T. A. Gabriel, and M. Blann, "Exerimental and Theoretical Study of the Yields of Radionuclides Produced in ^{209}Bi Thin Target Irradiated by 1500 MeV and 130 MeV Protons", *Nucl. Instr. and Meth*. **A414** (1998) 73-99.

[2] Yu. E. Titarenko, O. V. Shvedov, V. F. Batyaev, E. I. Karpikhin, V. M. Zhivun, A. B. Koldobsky, R. D. Mulambetov, D. V. Fischenko, S. V. Kvasova, A. N. Sosnin, S. G. Mashnik, R. E. Prael A. J. Sierk, T. A. Gabriel, M. Saito, and H. Yasuda, "Cross Sections for Nuclide Production in 1 GeV Proton-irradiated Pb," Los Alamos National Report LA-UR-00-4779, Los Alamos (2000), E-print nucl-th/0011083, submitted to Phys. Rev. C.

[3] K. K. Gudima, S. G. Mashnik, and V. D. Toneev, Nucl. Phys. **A401** (1983) 329; S. G. Mashnik, "User Manual for the Code CEM95", JINR, Dubna, 1995; OECD Nuclear Energy Agency Data Bank, Paris, France, 1995; http://www.nea.fr/abs/html/iaea1247.html; RSIC-PSR-357, Oak Ridge, 1995.

[4] V. S. Barashenkov, Le Van Ngok, L. G. Levchuk, Zh. Zh. Musul'manbekov, A. N. Sosnin, V. D. Toneev, and S. Yu. Shmakov, JINR Report R2-85-173, Dubna, 1985; V. S. Barashenkov, F. G. Zheregi, and Zh. Zh. Musul'manbekov, *Yad. Fiz.* **39** (1984) 1133 [*Sov. J. Nucl. Phys.* **39** (1984) 715]; V. S. Barashenkov, B. F. Kostenko, and A. M. Zadorogny, *Nucl. Phys.* **A338** (1980) 413.

[5] G. A. Lobov, N. V. Stepanov, A. A. Sibirtsev, and Yu. V. Trebukhovskii, ITEP Preprint ITEP-91, Moscow, 1983; A. A. Sibirtsev, N. V. Stepanov, and Yu. V. Trebukhovskii, ITEP Preprint ITEP-129, Moscow, 1985; N. V. Stepanov, ITEP Preprint ITEP-81, Moscow, 1987; N. V. Stepanov, ITEP Preprint ITEP-55-88, Moscow, 1988 (in Russian).

[6] R. E. Prael and H. Lichtenstein, "User Guide to LCS: The LAHET Code System," Los Alamos National Laboratory Report LA-UR-89-3014 (1989).

[7] C. H. Tsao, Private communication, R. Silberberg and C. H. Tsao, *Astrophys. J.* **220** (1973) 315; ibid 335.

[8] V. S. Barashenkov, A. Yu. Konobeev, Yu. A. Korovin, and V. N. Sosnin, *Atomnaya Energiya*, **87** (1999) 283.

[9] S. G. Mashnik and A. J. Sierk, "Improved Cascade-Exciton Model of Nuclear Reactions," in *Proceedings of the Fourth International Workshop on Simulating Accelerator Radiation Environments (SARE4), Knoxville, TN, 1998,* edited by T. A. *Gabriel*, (ORNL, 1999), p. 29.

[10] S. G. Mashnik and A. J. Sierk, "CEM2k – Recent Developments in CEM," Los Alamos National Laboratory Report LA-UR-00-5437, Los Alamos (2000); E-print nucl-th/0011064; to be published in *Proceedings of the 2000 ANS/ENS International Meeting, Nuclear Applications of Accelerator Technology (AccApp00),* November 12-16, 2000, Washington, DC, USA.

[11] S. G. Mashnik, L. S. Waters, and T. A. Gabriel, "Models and Codes for Intermediate Energy Nuclear Reactions," in *Proceedings of the Fifth International Workshop on Simulating Accelerator Radiation Environment (SARE5),* July 17-18, 2000, OECD Headquarters, Paris, France; LANL Report LA-UR-00-3775, http://bib-www.lanl.gov/la-pubs/00393746.pdf.

[12] J. R. Letaw et al. *Ap. J. Suppl*. **51** (1983) 271.

[13] A. Koning, "Nuclear Data Evaluation for Accelerator-Driven Systems", in *Proceedings of the Second International Conference on Accelerator-Driven Transmutation Technologies and Applications (ADTT'96)*, Kalmar, Sweeden, 1996, edited by H. Conde (Uppsala University, Uppsala, 1997), p. 438.

[14] W. Wlazlo, T. Enqvist, P. Armstrong, J. Benlliure, M. Bernas, A. Bouldar, S. Czajkowski, R. Legrain, S. Leray, B. Mustafa, M. Pravikoff, F. Rejmund, K.-H. Schmidt, C. Stephan, J. Taieb, L. Tassan-Got, and C. Volant, Phys. Rev. Lett. **84**, (2000) 5736.

[15] *MCNPX™ User's Manual, Version 2.1.5*, edited by Laurie S. Waters, Los Alamos National Laboratory Report TPO-E83-G-X-00001 (1999).

[16] F. Atchinson, "Spallation and Fission in Heavy Metal Nuclei under Medium Energy Proton Bombardment" *Targets for Neutron Beam Spallation Source*, Jul-Conf-34, Kernforschungsanlage Julich GmbH (January 1980).

[17] M. Zoeller, Dissertation, Technischen Hochschule, Darmstadt, 1995

[18] Yu. E. Titarenko, O. V. Shvedov, V. F. Batyaev, V. M. Zhivun, E. I. Karpikhin, R. D. Mulambetov, D. V. Fischenko, S. V. Kvasova, S. G. Mashnik, R. E. Prael, A. J. Sierk, and H. Yasuda, "Study of Residual Product Nuclide Yields in 1.0 GeV Proton-irradiated 208-Pb and 2.6 GeV Proton-irradiated *nat*-W Thin Targets", *Fifth Specialists Meeting on Shielding Aspects of Accelerators, Targets and Irradiation Facilities (SATIF-5),* 18-21 July 2000, Paris, France; E-print nucl-ex/0008011, LANL Report LA-UR-00-3597.

[19] Yu. E. Titarenko, O. V. Shvedov, V. F. Batyaev, V. M. Zhivun, E. I. Karpikhin, R. D. Mulambetov, D. V. Fischenko, S. V. Kvasova, S. G. Mashnik, R. E. Prael, A. J. Sierk, and H. Yasuda, "Study of Residual Product Nuclide Yields from 0.1, 0.2, 0.8, and 2.6 GeV Proton-Irradiated *nat*-Hg Targets," *Fifth Specialists Meeting on Shielding Aspects of Accelerators, Targets and Irradiation Facilities (SATIF-5),* 18-21 July 2000, Paris, France; E-print nucl-ex/0008012, LANL Report LA-UR-00-3600.